Future evolution of the hydroclimatic conditions favouring floods in the south-east of Belgium by 2100 using a regional climate model

Coraline WYARD, Chloé SCHOLZEN, Sébastien DOUTRELOUP, Éric HALLOT, Xavier FETTWEIS

Short title: Future evolution of hydroclimatic conditions favouring floods

Affiliations and address

C. WYARD

Remote Sensing and Geodata Unit

Institut Scientifique de Service Public

Rue du Chéra 200, 4000 Liège; Belgium

Tel: +32 4 2298316

c.wyard@issep.be

and

Laboratory of Climatology and Topoclimatology

University of Liège

Quartier Village 4, Clos Mercator 3, 4000 Liège, Belgium

Tel: +32 4 3669158

This article has been accepted for publication and undergone full peer review but has not been through the copyediting, typesetting, pagination and proofreading process which may lead to differences between this version and the Version of Record. Please cite this article as doi: 10.1002/joc.6642

C. SCHOLZEN

Department of Geosciences, University of Oslo, Norway

S. DOUTRELOUP and X. FETTWEIS

Laboratory of Climatology and Topoclimatology, Department of Geography, UR SPHERES, University of Liège, Belgium

É. HALLOT

Remote Sensing and Geodata Unit, Institut Scientifique de Service Public (ISSeP), Liège, Belgium

This research is funded by the Fund for Research Training in Industry and Agriculture from the F.R.S. – FNRS, Belgium.

Abstract: In Belgium, most flood events occur in winter as a result of intense precipitation events but also through the abrupt melting of the snowpack that covers the Ardennes summits. These conditions favourable to floods exhibit a decreasing trend over 1959–2010 resulting from the reduction in snow accumulation, although extreme precipitation events show a positive, albeit non-significant signal. In this study, the evolu-

tion of these trends in warmer climates is investigated by using future projections performed with the regional climate model MAR ("Modèle Atmosphérique Régional") forced by two global models NorESM1-M and MIROC5 under the RCP8.5 scenario. These models were selected from the CMIP5 archive after evaluation of their ability to represent the current (1976-2005) mean climate over Europe. By the end of the century, the results show an acceleration of the snow depletion resulting in fewer snowmelt-associated flood risk days depending on the warming rate from the AOGCM forcing MAR. Regarding the impact of the evolution of extreme precipitation events on hydro-climatic conditions favouring floods, no significant change was found although these trends are subject to uncertainties due to model physics and natural variability.

KEYWORDS: regional climate models ; CMIP5 ; Europe ; Belgium ; Ourthe ; floods ; snow ; precipitation

1. Introduction

Flow regimes in Belgian catchments are generally dominated by rainfall (pluvial) rather than snowfall, although snowmelt can be a major component of the regime for catchments that drain the Ardennes massif such as the Ourthe catchment. The Ourthe River is one of the main tributaries of the Meuse River, with a catchment area of about 3500 km² (Pauquet and Petit, 1993). While the Ourthe River is mainly rain-fed, the snowpack that

covers the Ardennes summits during winter also influences its discharge due to its buffering effect (Driessen et al., 2010). The Ourthe River reaches its peak either in winter or in spring when the snowpack is melting. In the Ourthe catchment, 70% of flood events occur during the winter months (December, January and February) (Wyard et al., 2017). About half of the observed floods are due to abundant rainfall alone. However, the rapid melting of the snowpack in the Ardennes, combined with heavy rainfall events, are responsible for major floods in the lower part of the Ourthe River, as it was the case in February 1984, March 1988, December 1991 and more recently, in January 2002 and January 2011 (Pauquet and Petit, 1993 ; de Wit et al., 2007). In a changing climate, hydroclimatic conditions favouring floods in the Ourthe catchment are therefore likely to be affected by changes in both snow cover and precipitation amount.

Global warming is already affecting snow and ice processes by reducing the amount of snowfall, the extent of the annual average snow cover and snow depth, and by inducing earlier snowmelt in various European regions such as the Alps (Durand et al., 2009 ; Valt and Cianfarra, 2010 ; Beniston, 2012), Britain (Kay, 2016), Norway (Skaugen et al., 2012 ; Dyrrdal et al., 2013), or Eastern Europe (Falarz, 2004 ; Brown and Petkova, 2007 ; Birsan and Dumitrescu, 2014). This declining snow cover is responsible for a decrease in the intensity and in the frequency of the floods dominated by snowmelt, which is predicted to accelerate in the future (Madsen et al., 2014; Bell et al., 2016; Vormoor et al., 2016). Belgian highlands are no exception to the trend, since their cur-

rent mean winter temperatures, just close to the freezing point, imply that they will be more affected by rising temperatures than colder or warmer regions (Hamlet and Lettenmaier, 2007 ; Stewart, 2009). By the use of modelling, Wyard et al. (2017) found that for the Ardennes the maximum snow height lowered by 5 to 15 cm/52 yrs over 1959-2010. Further, the number of days with at least 5 cm of snow accumulation declined by up to -15 days/52yrs, and in the highest parts of the Ourthe catchment the onset of the snow season was delayed by up to -60 days with respect to the 1960s. The consequence of such a decline in the Belgian seasonal snow cover is a significant decrease in snowmelt driven floods by -0.1 days winter^{-1} over 1959-2010 (Wyard et al., 2017). It should be noted that this declining snow cover may also affect water management, biodiversity, and tourism activities of High Belgium.

Regarding precipitation amount and extremes during winter, studies based either on observations (Gellens, 2000; Vaes et al., 2002; De Jongh et al., 2006; Ntegeka and Willems, 2008; Willems et al., 2013a, b; RMIB, 2015) or modelling (Wyard et al., 2017) found no significant long-term trend over the last century in any part of the Belgian territory. Nevertheless, these studies identify multidecadal oscillations characterized by drier periods in the 1900s, around 1920 and in the mid-1970s (De Jongh et al., 2006; Willems, 2013a,b), alternating with wetter periods in the 1910-1920s, the 1950-1960s and in the 1990-2000s (Ntegeka and Willems, 2008; Willems, 2013a,b), that coincide with the decadal variations of the North Atlantic Oscillation (NAO). Accordingly, hy-

droclimatic conditions favourable to floods induced by heavy rainfall alone show no significant long-term trend in the Ourthe catchment over 1959-2010 (Wyard et al., 2017), yet follow the same decadal oscillations as the NAO. Natural variability in the large scale atmospheric circulation can therefore play an important role on the winter time climate response to increasing greenhouse gas concentrations.

In the future, despite large uncertainties due to the internal variability of the climate system (Hawkins and Sutton, 2009 ; 2011; Deser et al., 2012a ; 2012b ; Prein and Pendergrass, 2019), the decline in seasonal snow cover is predicted to continue while the global hydrological cycle is expected to intensify (Vaughan et al., 2013). For Belgium, studies using regional climate models (RCM) forced by ensemble simulations from the Coupled Models Intercomparison Project phase 5 (CMIP5) archive (Tabari et al., 2015) and by downscaled atmosphere-ocean general circulation models (AOGCM) (Brouwers et al., 2015; Saeed et al., 2017; Vanden Broucke et al., 2018) concluded that under the RCP8.5 scenario, the intensification of the hydrological cycle would lead to increasing precipitation amounts, as well as more frequent and more intense extreme precipitation events in winter by the end of the 21^{-st} century. For the Ourthe River, Driessen et al. (2010) concluded that "*towards the end of the century, all scenarios show a decrease in summer discharge, partially because of the diminished buffering effect by the snow pack, and an increased discharge in winter*". Regarding hydroclimatic conditions favouring floods in the Ourthe catchment, it is expected (despite the absence of high reso-

lution projections for snow cover in Belgium) that the decline due to the decreasing snow cover will continue in the future, while conditions favourable to floods due to abundant rainfall alone would increase significantly.

This study aims to assess the impact of climate change on the winter climate of Belgium and its consequences on hydroclimatic conditions favourable to floods in the Ourthe catchment. This investigation is achieved by using high-resolution projections of snow cover and precipitation. Such projections were obtained by downscaling two AOGCMs, NorESM1-M and MIROC5, from the CMIP5 archive using the MAR ("Modèle Atmosphérique Régional") RCM. By contrast to AOGCMs whose typical resolution is approximately 40-200 km, RCMs run over a limited area, with dedicated physics at finer spatial resolution (down to 5 km for MAR). The representation of orographic features is a key factor for the simulation of temperature, precipitation and snow as the latter depends on the 0 °C isotherm location and elevation. The orography of Belgium, which ranges from sea level to about 700 m a.s.l., is known to have a clear barrier effect on precipitation averages (Journée et al., 2015) and associated extremes (Brisson et al., 2011 ; Sneyers et al., 1989 ; Van Meijgaard, 1995 ; Van de Vyver, 2012 ; Wyard et al., 2017 ; Zamani et al., 2016). Moreover, snow processes are usually not accounted for in AOGCMs, whereas they are included in some RCMs such as MAR. The ability of MAR to simulate the current winter climate of Belgium in terms of seasonal snow cover, precipitation extremes and hydroclimatic conditions favouring floods has been eval-

uated in Wyard et al. (2017), showing that MAR allows the detection of more than 90% of the observed floods in the Ourthe catchment over 1974-2014.

This paper is organised as follows: Section 2 provides some methodological aspects such as the RCM MAR and its forcing data. Section 3 details the evaluation of MAR forced by two AOGCMs over 1976-2005 using historical runs, and assesses the evolution of the Belgian winter climate under the RCP8.5 scenario throughout the 21^{-st} century. More specifically, Section 3.4 presents the trends for the hydroclimatic conditions favouring floods in the Ourthe catchment. The results are then discussed in Section 4. Conclusions and prospects are finally reported in Section 5.

2. Methods

2.1 The MAR model

The RCM used in this study is the MAR model which, although being initially designed for polar regions (Gallée & Schayes, 1994) such as Greenland (Fettweis et al., 2013) or Antarctica (Kittel et al., 2018), was recently adapted and applied to the temperate climate of Belgium (Fettweis et al., 2017 ; Wyard et al., 2017; 2018; Doutreloup et al., 2019a ; 2019b). MAR is a hydrostatic primitive equation model in which convection is parametrized according to Bechtold *et al.* (2001). The atmospheric part of MAR is fully described in Gallée & Schayes (1994), and Gallée (1995). Furthermore, MAR is coupled to the 1-D surface vegetation atmosphere transfer scheme SISVAT (Soil Ice Snow

Vegetation Atmosphere Transfer) which is detailed in De Ridder & Gallée (1998). The snow-ice part of SISVAT is the snow model CROCUS from the CEN (Centre d'Etudes de la Neige) described in Brun *et al.* (1992). The MAR-SISVAT coupling allows the consideration of three sub-pixel surface characteristics for a given MAR pixel. The coupling also allows interaction between surface and atmosphere (energy and moisture transfers), snow accumulation and snow melting on the surface, water percolation into the soil/snow, and run-off of exceeding water.

Simulations were performed at a resolution of 5 km over a domain of 120x110 pixels centred on (4.3°W ; 50.4°N) (see Figure S1). Boundary conditions (temperature, wind, humidity and pressure at each vertical level of MAR, and sea surface temperature) were provided every six hours to MAR from reanalyses or global models. In this study, the version 3.8 of MAR is used as in Wyard et al. (2018). Compared with MARv3.6, which was used in Wyard et al. (2017), MARv3.8 delays the onset of precipitation and hence increases the cloud cover which was underestimated in MARv3.6 (Wyard et al., 2017). In addition, in order to reduce the warm bias found in MARv3.6 in summer, the convective scheme is called twice as often in MARv3.8 than in MARv3.6, so that convective clouds can reside longer in the atmosphere before precipitating (Fettweis et al., 2017 ; Wyard et al., 2018). Finally, in MARv3.8 the vegetation seasonality is also better represented by using daily Leaf Area Index (LAI) and Green Leaf Fraction (GLF) from the MERRA-2 reanalysis (Gelaro et al., 2017), as opposed to MARv3.6 which used month-

ly values.

2.2 Forcing data

The simulations performed using MAR are listed in Table 1. Projections (2071-2100) under the RCP8.5 scenario were obtained by initializing the boundaries of MAR with output from two AOGCMs: the Norwegian Climate Center's Earth System Model (NorESM1-M) (Bentsen *et al.*, 2013; Iversen *et al.*, 2013), and the Japanese research community's Model for Interdisciplinary Research On Climate Version Five (MIROC5) (Watanabe *et al.*, 2010). These simulations are referred to as MAR-NOR-rcp85 and MAR-MIR-rcp85 hereafter.

For the historical period (1976-2005), simulations were also performed using the ERA-Interim reanalysis from the European Centre for Medium-Range Weather Forecasts (ECMWF) as lateral boundary conditions, with the aim of having a reference simulation against which the output of MAR forced by the two AOGCMs can be compared. These simulations are referred to as MAR-ERA, MAR-NOR-histo, and MAR-MIR-histo hereafter.

Both NorESM1-M and MIROC5 were selected from the CMIP5 multi-model archive (https://pcmdi.llnl.gov/), World Climate Research Program's (WCRP's) coordinated experimental framework which provided the standardized model dataset for the IPCC

fifth Assessment Report (AR5). Further information regarding the CMIP5 protocol can be found in Taylor et al. (2012).

2.3 CMIP5 AOGCM selection

For this study, NorESM1-M and MIROC5 were selected because they were identified as part of the most suited AOGCMs to represent the current mean (1976-2005) climate over Europe. It is well known that the ability of a GCM to model the general atmospheric circulation and surface conditions must be assessed before downscaling (e.g. Brands et al., 2013; Perez et al., 2014; McSweeney et al., 2015). The assessment of suitable CMIP5 models was conducted by comparing all ~30 CMIP5-AR5 models applying the 'skill score' methodology. The statistical classification used and discussed by Connolley and Bracegirdle (2007), and based on the probabilistic approach of Murphy *et al.* (2004), aims to measure the likelihood of a model to being within the range of the observations. First, a value is calculated for the root mean square (RMS) deviation of the multi-annual (1976-2005) averaged model field from the multi-annual observed field (based on ERA-Interim here), before being normalised by a measure of the variability of the field. This normalized value (RMS_n) is then rescaled into a weight (W) via the equation:

$$W = \exp(- 0.5 \times RMS_n^2)$$

W represents a 'score' between 0 and 1, which can be regarded an estimate of the AOGCM 'skill' to adequately simulate the climatological mean state over the consid-

ered period.

Skill scores were calculated for a number of climate variables, which were selected to represent the free atmosphere behaviours impacting the MAR results at its lateral boundaries (Table S1): 500 hPa wind speed (UV500), 700 hPa wind speed (UV700), 500 hPa geopotential height (Z500), 700 hPa geopotential height (Z700), 850 hPa air temperature in winter ($T_{JF}850$), and 850 hPa air temperature in summer ($T_{JJA}850$). Following the methodology of Murphy *et al.* (2004), RMS is normalized globally rather than pointwise, i.e. the spatial average of the RMS is scaled by the spatial average of the observations temporal variability. As pointed out by Connolley and Bracegirdle (2007), all the aforementioned choices imply that the method cannot be fully objective. Nonetheless, this approach provides the advantage of rating the models in terms of individual variables, which facilitates the choice of selecting one model over another, depending on the use case of the models and what aspect of the climate is analyzed. Agosta et al. (2015) showed that the ranking of the CMIP5 AOCGMs was not significantly influenced by multi-decadal variability. Our skill score analysis revealed that, despite a strong variability among the skill scores, NorESM1-M and MIROC5 skill scores are among the highest (Table S1). In addition, these two AOGCMs have the advantage that the MAR preprocessing tool was already adapted to their outputs (Fettweis et al., 2013 ; Lang et al., 2015).

2.4 Hydroclimatic conditions favourable to floods

Hydroclimatic conditions favouring floods were computed for the Ourthe catchment upstream of Sauheid (see Figure S1). This part of the catchment has an area of 2900 km² and its limits are drawn in dark blue in Figure 1 to Figure 4 and in Figure S1 to Figure S5 (see Supporting Information).

As explained in Wyard et al. (2017), a day was defined as favourable to floods if the run-off computed by MAR, integrated and averaged over the Ourthe catchment area and finally averaged over the two days preceding the flood event, is larger than its 95th percentile computed over the 30-year reference period (1976-2005). In fact, the use of this criterion has allowed to detect up to 90% of the hydroclimatic conditions which effectively generated observed floods in the Ourthe River over the period 1974-2014 (Wyard et al., 2017). In addition, the distinction between extreme run-off events generated by snowmelt combined with rainfall (SFD for Snowmelt-dominated Flood Days) and extreme run-off events generated by heavy rainfall only (RFD for Rainfall-dominated Flood Days) was applied. The total number of days favourable to floods (TFD) is the sum of SFD and RFD.

3. Results

The first aim of this section is to evaluate the ability of MAR forced by two AOGCMs selected from the CMIP5 archive, NorESM1-M and MIROC5, to simulate the present-day climate over Belgium during the winter months (December, January, and February).

A good representation of the current climate is a necessary condition to reliably and more realistically simulate future climate change, since the response of the climate variables to a warming is not linear and could be impacted by their biases over current climate (Fettweis et al., 2013). In order to evaluate the reliability of MAR forced by NorESM1-M and MIROC5, the climatic mean of both MAR-NOR-histo and MAR-MIR-histo is compared to MAR-ERA over 1976-2005 by evaluating temperature, precipitation, snow cover and conditions favourable to floods.

The second aim is to assess the evolution of the Belgian climate during the winter months by the end of the 21^{-st} century under the RCP8.5 scenario. Changes in the future Belgian climate were assessed by comparing the 2071-2100 mean winter climate computed by MAR-NOR-rcp85 and MAR-MIR-rcp85 to the 1976-2005 mean winter climate computed by MAR-NOR-histo and MAR-MIR-histo.

As previously done in Fettweis et al. (2013) and in IPCC AR5, the significance of anomalies over current climate was assessed by comparing them to the interannual variability (standard deviation) of MAR-ERA over 1976-2005, while the significance of projected changes was assessed by comparing them to the interannual variability of MAR-NOR-histo and MAR-MIR-histo over 1976-2005. These statistical tests are t-test at 0.1 level of significance because temperature and precipitation can be regarded as normally distributed quantities, as shown by Dupriez & Sneyers (1978) or De Jongh et

al. (2006).

3.1 Winter temperature

The seasonal climatology of the mean winter temperature and the number of winter frost days computed over 1976-2005 from MAR-ERA is displayed in Figure S2. Compared to this reference climatology, MAR-NOR-histo significantly overestimates mean winter temperature by up to +3 °C (Figure 1(a)). Such anomalies are large compared to the 1976-2005 mean winter temperature simulated by MAR-ERA, which ranges from -1 to 4 °C (Figure S2(a)). The number of winter frost days, defined as the number of days with daily minimum temperature below 0 °C, is significantly underestimated in MAR-NOR-histo by -10 days $winter^{-1}$ in Low Belgium (part of the country where elevation above sea level (z) does not exceed 100 m) and by -25 days $winter^{-1}$ in the highest parts of the Ardennes massif (Figure 1(b)). These anomalies are also large compared to the 1976-2005 winter frost days simulated by MAR-ERA, which range from 30 to 70 days $winter^{-1}$ (Figure S2(b)). MAR-MIR-histo, for its part, shows non-significant anomalies in mean winter temperature (Figure 1(c)), while the number of winter frost days is significantly overestimated in Low and Middle Belgium (part of the country where 100 m $< z <$ 300 m) by +10 to +15 days $winter^{-1}$ (Figure 1(d)).

For the end of the 21^{-st} century, MAR-MIR-rcp85 produces larger changes in temperature than MAR-NOR-rcp85 with respect to the present-day climate (Figure 1(e, g)), and

projected changes are larger than the anomalies over the present-day climate. The 2071-2100 mean winter temperature computed by MAR-NOR-rcp85 exhibits a significant increase by +3°C over the entire Belgian territory with respect to 1976-2005 (Figure 1(e)). These values range from +3 to +4.5 °C for MAR-MIR-rcp85 (Figure 1(g)) depending on the topography and, on the distance to the North Sea with shorter distances experencing smaller warming. The results also show a significant decrease in the number of winter frost days by -15 days winter^{-1} in coastal regions and by -25 days winter^{-1} in the highest parts of Belgium for MAR-MIR-rcp85 (Figure 1(h)). MAR-NOR-rcp85, for its part, exhibits a decrease between -10 and -20 days winter-1 (Figure 1(f)).

High-resolution simulations performed with COSMO-CLM and ALARO project more important changes (Brouwers et al., 2015). Under RCP8.5, these RCMs show a significant increase in mean winter temperature valued at +6.2°C for Uccle, Middle Belgium, by the end of the century.

3.2 Winter precipitation

Compared to MAR-ERA, MAR-NOR-histo is wetter while MAR-MIR-histo is drier over 1976-2005 (Figures 2 and S3). MAR-NOR-histo shows significant positive anomalies in total winter precipitation over the Ardennes massif, ranging from +40 to +140 mm winter^{-1} (Figure 2(a)), mainly due to an excess in rainfall (liquid part of total precipitation) (Figure 2(b)). Regarding the intensity of extreme precipitation events in winter

(the 95th percentile of the daily precipitation amount in winter as defined in Wyard et al. (2017)) and the frequency of extreme precipitation events in winter (the number of days with daily precipitation amount larger than its 95th percentile over 1976-2005), MAR-NOR-histo shows no significant bias in either of these two variables with respect to MAR-ERA (Figure S4(b, c)). By contrast, the amount of convective precipitation is overestimated in MAR-NOR-histo compared to MAR-ERA, with anomalies ranging from +10 to 50 mm winter^{-1} (Figure S4(a)). MAR-MIR-histo displays the opposite behaviour by simulating too little total winter precipitation over the entire Belgian territory except for coastal regions, with respect to MAR-ERA. These anomalies range from -20 to -160 mm winter^{-1} (Figure 2(d)) and result from a failure of MAR-MIR-histo to produce enough rainfall (Figure 2(e)). In terms of extreme precipitation event intensity, MAR-MIR-histo significantly underestimates it over the southern and the north-eastern parts of Belgium, with anomalies ranging from -1 to more than -6 mm day^{-1} (Figure S4(e)). It should be noted that the anomalies in total winter precipitation, rainfall and extreme event intensity are the largest in south-western foothills of the Ardennes massif, which is the direction from which most of the winter perturbations originate from. As temperature is underestimated in MAR-MIR-histo with respect to MAR-ERA (Figure 1(c)), this suggests that saturation is not reached in this part of the country due to a lack of humidity.

By comparing the 2071-2100 mean climate to the 1976-2005 mean climate, both MAR-

NOR-rcp85 and MAR-MIR-rcp85 agree on a significant decrease in the amount of snowfall (solid part of total precipitation) over the Ardennes massif, with values ranging from -20 to -80 mm winter^{-1} (Figure 2(i, l)). This represents a decrease from -50 to -70 % winter^{-1} compared to 1976-2005. This important depletion in snowfall is not counter-balanced by any substantial increase in rainfall, as both MAR simulations project no significant change in rainfall over the Ardennes massif (Figure 2(h, k)). MAR-NOR-rcp85 simulates significantly higher rainfall over coastal regions only, ranging from +40 to +70 mm winter^{-1} ,which represents an increase between +20 and +50 % winter^{-1} (Figure 2(h)). In addition, MAR-NOR-rcp85 and MAR-MIR-rcp85 also agree on significantly higher convective precipitation in winter, as shown in Figure S4(g, j), although the changes simulated by MAR-NOR-rcp85 are smaller than the anomalies over present-day climate (Figure S4(a, g)). Regarding changes in extreme precipitation events, only MAR-NOR-rcp85 simulates a significant increase in their intensity (from +10 to +40 %) and in their frequency (between +1 and +2 days winter-1, i.e. +40 to +80 % winter-1), and only over very limited parts of northern Belgium (Figure S4(h)) and coastal regions (Figure S4(i)), respectively.

Over western Europe, Aalbers et al., (2018) show that a regional downscaling of a 16-member initial-condition ensemble using the RCM RACMO2 driven by the GCM EC-EARTH 2.3 simulates a significant intensification of mean and extreme precipitation in winter (despite a strong internal variability). They also show that mean and extreme

precipitation increase with the same rate of change with global warming. Tabari et al. (2015) show that ensemble simulations from CMIP5 exhibit an increase in total winter precipitation valued at +19.62 ± 21.64 % over Belgium. Using high resolution future projections over Belgium, Brouwers et al. (2015) simulate an increase in total winter precipitation of +38 % winter^{-1} over central Belgium. These changes are in the range of the changes simulated by MAR-NOR-rcp85 (but non-significant over central Belgium). However, the significance of these changes is not discussed in both of the previously mentioned studies. As in MAR-NOR-rcp85, this increase is expected to be greater in coastal regions. Brouwers et al. (2015) stated that this coastal effect is greatly dependent on the interaction between changes in air currents, the temperature contrast between land and sea, and the increase in temperature. For instance, the models that predict the greatest increase in precipitation near the coast are also those with the greatest temperature gradient between the North Sea and land (Brouwers et al., 2015). According to MAR-NOR-rcp85, Saeed et al. (2017), using the COSMO-CLM RCM forced by the EC-EARTH model, simulated a significant increase (using a t-test at the 0.01 level of significance) in the intensity of extreme precipitation events by mid-century (2060-2069), which is predicted to continue beyond this period (Brouwers et al., 2015). Vanden Broucke et al. (2018) also found a significant increase (using a t-test at the 0.01 level of significance) in both the frequency and the intensity of extreme daily precipitation accumulation by the end of the 21^{-st} century. This amplification is again expected to be the largest in coastal regions. Compared to these studies, the changes in extreme pre-

cipitation events projected by MAR are less important. As discussed in Section 4.2, this may result from AOGCMs used to force RCMs and/or from limitations in the physics of MAR for simulation of convective precipitation.

3.3 Winter snow cover

Compared to the 1976-2005 climatology computed from MAR-ERA (Figure S5), both MAR-NOR-histo and MAR-MIR-histo show non-significant anomalies over most parts of Belgium (Figure 3). MAR-MIR-histo significantly overestimates daily mean and maximum snow height only over the lowest part of Belgium with anomalies ranging from +3 to more than +5 cm (Figure 3(d, e)), whereas MAR-ERA simulates average daily maximum snow height values up to 5 cm (Figure S5(c)). Since only rainfall anomalies are significant, and since the pattern of the anomalies in daily maximum snow height is comparable to the anomalies in winter frost days (Figure 1(d)), it may be concluded that the overestimation of daily maximum snow height over Low Belgium is mainly driven by the underestimation of temperature, reaching 0°C more often in MAR-MIR-histo than in MAR-ERA.

By the end of the century, MAR-MIR-rcp85, which simulates the largest temperature increase and the largest snowfall decrease, consequently projects a substantial depletion in snow cover (Figure 3(j, k, l)). MAR-MIR-rcp85 shows a significant drop in the daily mean snow height from -2 to -8 cm (Figure 3(j)), as well as in the daily maximum snow

height ranging from -2 to -6 cm over lowlands, and from -6 cm to more than -10 cm in the Ardennes (Figure 3(k)). The number of snow days (the number of days per winter with a snow cover of at least 5 cm of thickness) is also significantly decreasing over the highest parts of the Ardennes in MAR-MIR-rcp85 by 2100, with values larger than -10 days winter^{-1} (Figure 3(l)). All these changes in snow cover simulated by MAR-MIR-rcp85 are larger than their anomalies over the present-day climate.

The decrease in these three variables probably results from the significant decline in snowfall simulated by MAR (Section 3.2), albeit Section 3.1 shows that warmer winter temperatures coherently lead to fewer winter frost days, while the accumulation of snow pack is only possible at temperatures below zero degrees Celsius.

3.4 Conditions favouring floods in winter

Finally, the ability of MAR forced by both AOGCMs to simulate hydroclimatic conditions favourable to floods in the Ourthe catchment (as defined in Section 2.4) is investigated. Table 2 shows that, when compared to the MAR-ERA interannual variability, both MAR-NOR-histo and MAR-MIR-histo exhibit non-significant anomalies in SFD (Snowmelt-dominating Flood Days), RFD (Rainfall-dominating Flood Days), and consequently TFD (total number of days favourable to floods; TFD=RFD+SFD). Therefore it is concluded that the significant anomalies found in precipitation and temperature in both MAR-NOR-histo and MAR-MIR-histo do not impact the simulation of extreme

run-off events in the Ourthe catchment in winter.

Regarding projected changes for the end of the century, the 2071-2100 SFD is valued at 1.2 days winter^{-1} in MAR-NOR-rcp85 and 1.8 days winter^{-1} in MAR-MIR-rcp85 (Table 3). Compared to 1976-2005, this represents a significant decrease of -73 % and -74 % respectively (Table 3), which results from lower daily maximum snow height and fewer winter snow days simulated in the Ardennes (Section 3.3). The evolution of SFD between 1976 and 2100 is plotted in Figure 4(a, d). Despite a large interannual variability, SFD declines steadily in both MAR future simulations. The linear trend in SFD for the period 2006-2100 is significant and valued at -0.023 days winter^{-1} in MAR-NOR-rcp85 (Figure 4(a)) and -0.024 days winter^{-1} in MAR-MIR-rcp85 (Figure 4(d)). The 2071-2100 RFD is valued at 8.3 days winter^{-1} in MAR-NOR-rcp85 and 4.8 days winter^{-1} in MAR-MIR-rcp85 (Table 3). Compared to 1976-2005 (Table 3), this represents a non-significant gain of +26% and +39% respectively (Table 3), which is due to a non-significant increase in rainfall, extreme precipitation event intensity and frequency simulated in the Ardennes (Section 3.2). The linear trend in RFD for the period 2006-2100 is also non-significant. The resulting 2071-2100 TFD is valued at 9.5 days winter^{-1} in MAR-NOR-rcp85 and 6.6 days winter^{-1} in MAR-MIR-rcp85 (Table 3). Compared to 1976-2005 (Table 3), this represents a loss of -13% and -37% respectively, which is statistically significant in MAR-MIR-rcp85 only (Table 3). This negative trend of TFD is evidently dominated by the decrease in SFD.

4. Discussion

Section 3 has brought to light discrepancies between MAR forced by NorESM1-M and MAR forced by MIROC5 which need to be explained. The comparisons of MAR-NOR-histo and MAR-MIR-histo with MAR-ERA reveal that the simulations forced by the two AOGCMs exhibit opposite anomalies. MAR-NOR-histo is on average too warm and too wet, while MAR-MIR-histo is too cold and too dry but with too much snow with respect to MAR-ERA. Regarding projected changes under the RCP8.5 scenario, both models generally agree on warming temperatures, rising rainfall and convective precipitation, declining decreasing daily maximum snow height and fewer winter snow days by the end of the century. Consequently, both models simulate a decrease in SFD and a (non-significant) increase in RFD in the Ourthe catchment. However, the temperature rise in MAR-MIR-rcp85 is 2°C larger than in MAR-NOR-rcp85, which leads to a larger reduction in snowfall and in snow cover than in MAR-NOR-rcp85. The latter simulation shows a larger increase in rainfall, convective precipitation and in extreme precipitation events intensity and frequency than MAR-MIR-rcp85.

4.1. Uncertainties in the AOGCM forcings

Since all MAR simulations performed in this study use exactly the same MAR setup, it may be concluded that the discrepancies between these MAR simulations can only be

explained by their boundary forcings. Inherent biases in the CMIP5 AOGCMs have been widely investigated in the literature. By comparing NorESM1-M with observations and reanalyses over 1976-2005, Bentsen et al. (2013) highlight that NorESM1-M overestimates cloud liquid water content (and thus precipitation and humidity), particularly in the extratropical storm track regions. Bentsen et al. (2013) also found that the model produces too warm air temperatures over Western Europe. These biases are in agreement with the overestimation of rainfall and winter near-surface air temperature over Belgium found in MAR-NOR-histo. Watanabe et al. (2010) compared MIROC5 to observational data, reanalyses and other global models, and thereby showed that the model produces slightly too little precipitation, which is in agreement with the underestimated winter precipitation found in MAR-MIR-histo, while MAR is only forced by humidity at its lateral boundaries. In this study, comparison between the trends computed from the MAR future projections and the trends computed from NorESM1-M and MIROC5 regarding rainfall and snowfall confirms indeed that the differences between both our MAR simulations result from inconsistencies in their lateral forcing (Figure S6).

4.2. The role of natural variability

Opposite patterns in individual ensemble members have been shown to originate from internal variability in the large scale circulation (Kjellström et al., 2013 ; Deser et al., 2017). The European wintertime climate is strongly constrained by the occurrence and the persistence of quasi-stationary circulation patterns of larger scale, also referred to as

"weather regimes" (Reinhold and Pierrehumbert, 1982; Legras and Ghil, 1985; Vautard, 1990). Anomalies in the frequency of occurrence of each weather regime simulated by the AOGCMs could therefore be responsible for the anomalies found in our MAR simulations. Studies usually classify these circulation patterns in four categories (Cassou, 2008; Cattiaux et al, 2010; 2013). The positive phase of the NAO (NAO+) is generally associated with mild and rainy winters over Belgium, while the negative phase of the NAO (NAO-) is associated with cold and snowy winters. The persistence of a high-pressure system over Northern Europe or the British Isles, often referred to as “Scandinavian blocking” (SB) conditions, leads to cold and dry weather over Western Europe. By contrast, the persistence of a high-pressure system over the Northern Atlantic, also referred to as "Atlantic ridge" (AR), allows inflow of Arctic maritime air over Europe and is associated with cold and snowy winters. Cattiaux et al. (2013) investigated the ability of each CMIP5 AOGCM to simulate the present-day mean frequencies of occurrence of all four circulation patterns in winter over Europe. For the period 1979-2008, NorESM1-M overestimates the NAO+ mean frequency by about +18 %, while underestimating the NAO- and the SB mean frequencies by about -5 % and -15 % respectively. This is fully consistent with the positive anomalies in temperature and (liquid) precipitation, as well as the negative anomalies in snow accumulation of MAR-NOR-histo over a similar period (1976-2005) compared to MAR-ERA. MIROC5, however, overestimates the NAO- and the AR mean frequencies by about +20 % and +10 % respectively, while underestimating the NAO+ and the SB mean frequencies by about -25 % and -5

% respectively. This is in agreement with the negative anomalies in temperature and (liquid) precipitation, as well as the positive anomalies in snow accumulation of MAR-NOR-histo (1976-2005) with respect to MAR-ERA. Cattiaux et al. (2013) also compared the 2071-2100 mean frequencies of occurrence of the main weather regimes simulated by the CMIP5 AOGCMs with their 1981-2010 mean frequencies. They found that NorESM1-M exhibits more frequent AR regime (+5%) and NAO- regime (+3%), whereas MIROC5 produces more frequent NAO- regime (+8%) and NAO+ regime (2%) in the future. The higher occurrence of NAO+ regime in MIROC5 may therefore explain the larger increase in winter temperature simulated by MAR-MIR-rcp85.

4.3. Model sensitivity to RCP scenarios

RCM projections are also inevitably affected by the choice of the gas emission scenario. The sensitivity of our MAR future simulations is likely even higher considering that our analysis focuses on the end of the century where divergence between RCP scenarios is larger than in a shorter time horizon. Moreover, choosing the pathway with the highest radiative forcing (RCP 8.5) certainly magnifies its impact on our findings, since the hydroclimatic issue addressed in this study (snowmelt driven flood risk) is highly sensitive to warming temperatures. Nevertheless, several studies seem to suggest that RCM projections are less sensitive to RCP scenarios than to AOGCM internal climate variability. Van Uytven et al. (2018) analysed 160 CMIP5 climate simulations and demonstrated that for the time horizon 2071-2100, the AOGCM uncertainty overpasses the uncertain-

ty linked to the greenhouse gas concentrations. Findings of Deser et al. (2012a, b) had already highlighted that the dominant source of uncertainty in the simulated climate response at middle and high latitudes is internal atmospheric variability associated with large scale circulation variability. Von Trentini et al. (2019) stated that, although the contribution of internal variability to ensemble projection variability significantly decreases over time, in the far future for most regions and seasons internal variability explains 25–75% of the overall variability. Our findings seem to support that the contribution of RCP scenario choice to model projection uncertainty is relatively less important than AOGCM internal variability. Comparison of the MAR projections to existing literature has shown that other RCMs, using different AOGCMs as forcings, project more intense warming and larger changes in extreme precipitation events (see Sections 3.1 and 3.2), despite using the same greenhouse gas emission scenario (RCP 8.5). Cattiaux et al. (2012) also found that, under the same RCP scenario, both NorESM-1M and MIROC5 yield indeed a different increase in temperature, which is consistent with our findings, as MAR-MIR-rcp85 projects higher warming than MAR-NOR-rcp85 and hence more strongly affects the balance of snow related flood risk in the future.

4.4. Uncertainties linked to convection parameterization

Besides uncertainties related to emission scenarios and natural variability in the AOGCMs, parameterizations implemented in the MAR RCM provide an additional source of uncertainty in our future projections. The comparison of winter precipitation

changes with existing literature (Section 3.2) has shown that MAR seems to underestimate changes in extreme precipitation event intensity. Therefore, despite the significant improvements implemented in the convective scheme of MARv3.8 (Fettweis et al., 2017; Wyard et al., 2018), substantial biases remain in the simulation of convective precipitation. Doutreloup et al. (2019a, 2019b) tested the sensitivity of MARv3.9 to five different convective schemes and concluded that none of these convective schemes significantly improves the representation of convective precipitation events. Given the projected increase in convective winter precipitation, using a non-hydrostatic RCM could provide some improvement to the reliability of the projected wintertime precipitation, although the role of convective precipitation remains very limited in the winter months compared to other types of precipitation.

5. Conclusion

The main objectives of this paper were first to quantify the future evolution of the winter Belgian climate and especially of its seasonal snow cover by the end of the 21^{-st} century under the RCP8.5 scenario. Secondly, since most of the floods that take place in the Ardennes rivers occur in winter as a result of rapid snowpack melting and/or heavy rainfall events, this paper also aimed to assess the consequences of these changes on hydroclimatic conditions favouring winter floods in the Ourthe catchment. For this purpose, two AOGCMs from CMIP5, NorESM1-M and MIROC5, were dynamically downscaled using the MAR RCM. Historical simulations (MAR-NOR-histo and MAR-MIR-histo)

and future projections (MAR-NOR-rcp85 and MAR-MIR-rcp85) were then performed using version 3.8 of MAR forced by these two AOGCMs. Historical simulations were evaluated by comparing MAR-NOR-histo and MAR-MIR-histo to MAR forced by the ERA-interim reanalyses (MAR-ERA) for the period 1976-2005 with focus on the winter months (DJF). An evaluation of future trends in the Belgian winter climate was carried out by comparing the 2071-2100 mean future climate to the 1976-2005 mean present-day climate.

The evaluation of the MAR forced by AOGCM simulations has brought to light anomalies of opposite sign arising from the forcings. MAR-NOR-histo is on average warmer and wetter in winter than MAR-ERA, while MAR-MIR-histo is colder, drier and more snowy. For instance, MAR-NOR-histo significantly overestimates mean winter temperature up to +3°C, while MAR-MIR-histo exhibits negative but non-significant anomalies in mean winter temperature. Significant anomalies are also found in precipitation. MAR-NOR-histo overestimates rainfall up to +140 mm winter^{-1} on the Ardennes summits, while MAR-MIR-histo underestimates rainfall up to -140 mm winter^{-1} in the south-western foothills of the Ardennes. No significant anomalies are found in snow accumulation except in MAR-MIR-histo which significantly overestimates daily maximum snow height in the coastal regions. Regarding hydroclimatic conditions favouring floods in the Ourthe catchment, discrepancies between MAR-ERA, MAR-NOR-histo, and MAR-MIR-histo are found to be non-significant.

Future trends confirm that the current observed trends (Wyard et al., 2017) in the Belgian winter climate will continue under a warming climate. By comparing the 2071-2100 mean climate to 1976-2005, both MAR-NOR-rcp85 and MAR-MIR-rcp85 agree on future increasing temperature (up to +5°C in MAR-MIR-rcp85), increasing convective precipitation (up to +50 mm winter^{-1} in MAR-NOR-rcp85) and decreasing snowfall (up to -80 mm winter^{-1} in MAR-MIR-rcp85), daily maximum snow height (more than -10 cm winter^{-1} in MAR-MIR-rcp85) and number of winter snow days (more than -10 days winter^{-1} in MAR-MIR-rcp85). Only MAR-NOR-rcp85 shows a significant increase in rainfall, although only in the coastal regions. It should also be noted that MAR-MIR-rcp85 shows a larger increase in temperature and a larger decrease in the snow cover than MAR-NOR-rcp85, while the latter exhibits a stronger rise in convective precipitation and rainfall. As a consequence of these changes in the winter climate projected by MAR, a significant decrease in SFD and a (non-significant) increase in RFD are found in the Ourthe catchment. Compared to 1976-2005, the 2071-2100 mean SFD decreases by about -70%, while RFD is increasing by +26% in MAR-NOR-histo and by +39% in MAR-MIR-rcp85. As a result, TFD shows no significant trend.

This study provides the first quantified projections of the seasonal snow cover of Belgium. Given the importance of the seasonal snow cover for flood risk, water management, biodiversity and tourism activities of High Belgium, quantification of changes in

snow cover is important for the assessment of their hydrological, ecological and economical impacts.

In addition, this study underlines the sensitivity of the RCM results to their forcing AOGCMs. Under the same RCP scenario, the AOGCM driving the RCM influences the amount of warming and the large-scale circulation changes affecting the balance of snow-related processes. This suggests that both the natural variability of climate and the emissions pathways are crucial to the character of future flood risk. Hence, a conclusion from only two AOGCM forcing simulations remains difficult, as the AOGCMs used in this study may not span the range of realistic future temperature changes.

Finally, shortcomings in the parameterization of convection add uncertainty to the reliability of changes in the amount of precipitation, in extreme precipitation event intensity and frequency. As a consequence, changes in flood risk due to abundant rainfall may remain unquantified.

As further perspectives, given that part of the uncertainties found in our simulations are inherited from the forcing AOGCMs, it may be relevant to reiterate this study with the updated forcing data (CMIP6), so as to assess the sensitivity of our RCM MAR to the AOGCM uncertainty. Ensemble simulations may be performed in order to quantify the internal variability of the climate system and more robustly estimate the climate signal.

In addition, the same experiments may be performed using a non-hydrostatic RCM as the simulation of reliable convective precipitation could be needed to quantify changes in the flood risk due to abundant rainfall.

Acknowledgments: The authors acknowledge the Fonds pour la formation à la Recherche dans l'Industrie et dans l'Agriculture (FRIA) for funding this research. The authors are also grateful to the University of Liège (ULiège), the Institut Scientifique de Service Public (ISSeP) ,and the University of Oslo (UiO) for their support. In addition, the authors acknowledge the Consortium des Équipements de Calculs Intensifs (CECI) for providing high-performance scientific computing facilities and resources. ERA-Interim reanalysis used in this study were obtained from the ECMWF data server: http://apps.ecmwf.int/datasets, and the CMIP5 AOGCM outputs were obtained from https://esgf-node.llnl.gov/projects/cmip5/**.**

Supporting information

Table S1. Skill scores for six atmospheric variables: 500 hPa and 700 hPa wind speed (UV500, UV700), 500 hPa and 700 hPa geopotential height (ZG500, ZG700), 850 hPa winter (January-February) and summer (June-July-August) air temperature (TJF850, TJJA850).

Figure S1. The 120x110-pixel integration domain of MAR for the 5-km space grid centred on (4.3°W;50.4°N) and its orography (elevation of the surface above sea level).

Figure S2. The 1976-2005 average **(a)** mean winter temperature, and **(b)** number of winter frost days, simulated by MAR forced by ERA40/ERA-interim during the winter months (December-January-February).

Figure S3. The 1976-2005 average **(a)** total precipitation amount, **(b)** convective precipitation amount, **(c)** rainfall amount, **(d)** snowfall amount, **(e)** extreme precipitation intensity, and **(f)** extreme precipitation frequency, simulated by MAR forced by ERA40/ERA-interim during the winter months (December-January-February).

Figure S4. (Top) Present-day anomalies of MAR forced by NorESM1-M and MIROC5 with respect to MAR forced by ERA40/ERA-interim during the winter months (December-January-February) over 1976-2005 regarding **(a, d)** convective precipitation amount, **(b, e)** extreme precipitation intensity, and **(c, f)** extreme precipitation frequency. (Bottom) Future changes simulated by MAR forced by NorESM1-M and MIROC5 over 2071-2100 during the winter months (December-January-February) with respect to 1976-2005 regarding **(g, j)** convective precipitation amount, **(h, k)** extreme precipitation intensity, and **(i, l)** extreme precipitation frequency. Stippling pixels indicate anomalies/changes that are statistically significant with respect to the interannual variability of the reference field.

Figure S5. The 1976-2005 average **(a)** number of snow days, **(b)** daily mean snow height, and **(c)** daily maximum snow height, simulated by MAR forced by ERA40/ERA-interim during the winter months (December-January-February).

Figure S6. Changes in winter (DJF) simulated by NorESM-1M and MIROC5 over 2071-2100 with respect to 1976-2005 regarding **(a, c)** the amount of rainfall, and **(b, d)** the amount of snowfall. Stippling pixels indicate anomalies/changes that are statistically non-significant with respect to the interannual variability of the reference field.

References

Agosta C, Fettweis X, Datta R. 2015. Evaluation of the CMIP5 models in the aim of regional modelling of the Antarctic surface mass balance. The Cryosphere 9(6): 2311-2321. DOI: 10.5194/tc-9-2311-2015

Aalbers EE, Lenderink G, van Meijgaard E, van den Hurk BJ. 2018. Local-scale changes in mean and heavy precipitation in Western Europe, climate change or internal variability?. Climate Dynamics 50(11-12): 4745-4766. DOI: 10.1007/s00382-017-3901-9.

Bechtold P, Bazile E, Guichard F, Mascart P, Richard E. 2001. A mass-flux convection scheme for regional and global models. Quarterly Journal of the Royal Meteorological Society 127(573): 869–886. DOI: 10.1002/qj.49712757309.

Bell VA, Kay AL, Davies HN, Jones RG. 2016. An assessment of the possible impacts of climate change on snow and peak river flows across Britain. Climatic Change 136(3–4): 539–553. DOI: 10.1007/s10584-016-1637-x.

Beniston M. 2012. Is snow in the Alps receding or disappearing? Wiley Interdisciplinary Reviews: Climate Change 3(4): 349–358. DOI: 10.1002/wcc.179.

Bentsen M, Bethke I, Debernard JB, Iversen T, Kirkevåg A, Seland Ø, Drange H, Roelandt C, Seierstad IA, Hoose C, Kristjánsson JE. 2013. The Norwegian Earth System Model, NorESM1-M – Part 1: Description and basic evaluation of the physical climate. Geoscientific Model Development 6(3): 687–720. DOI: 10.5194/gmd-6-687-2013.

Birsan M, Dumitrescu A. 2014. Snow variability in Romania in connection to large-scale. International Journal of Climatology 34: 134–144. DOI: 10.1002/joc.3671.

Brands S, Herrera S, Fernández J, and Gutiérrez JM. 2013. How well do CMIP5 Earth System Models simulate present climate conditions in Europe and Africa?: A performance comparison for the downscaling community. Climate Dynamics 41 (3-4): 803-817. DOI: 10.1007/s00382-013-1742-8.

Brisson E, Demuzere M, Kwakernaak B, Van Lipzig NPM. 2011. Relations between atmospheric circulation and precipitation in Belgium. Meteorology and Atmospheric Physics 111(1–2): 27–39. DOI: 10.1007/s00703-010-0103-y.

Brouwers J, Peeters B, Van Steertegem M, van Lipzig N, Wouters H, Beullens J, Demuzere M, Willems P, Ridder K De, Maiheu B, Troch R De, Termonia P, Vansteenkiste T, Craninx M, Maetens W, Defloor W, Cauwenberghs K. 2015. MIRA Climate Report 2015, about observed and future climate changes in Flanders and Belgium. Flanders Environment Agency in collaboration with KU Leuven, VITO and RMI. DOI: 10.13140/RG.2.1.2055.8809.

Brown RD, Petkova N. 2007. Snow cover variability in Bulgarian mountainous regions, 1931–2000. International Journal of Climatology 27(9): 1215–1229. DOI: 10.1002/joc.1468.

Brun É, David P, Sudul M, Brunot G. 1992. A numerical model to simulate snow-cover stratigraphy for operational avalanche forecasting. Journal of Glaciology 38(128): 13–22.

Cassou C. 2008. Intraseasonal interaction between the Madden–Julian Oscillation and the North Atlantic Oscillation. Nature 455(7212): 523–527. DOI: 10.1038/nature07286.

Cattiaux J, Douville H, Peings Y. 2013. European temperatures in CMIP5: origins of present-day biases and future uncertainties. Climate Dynamics 41(11–12): 2889–2907. DOI: 10.1007/s00382-013-1731-y.

Cattiaux J, Vautard R, Cassou C, Yiou P, Masson-Delmotte V, Codron F. 2010. Winter

2010 in Europe: A cold extreme in a warming climate. Geophysical Research Letters 37(20): L20704 . DOI: 10.1029/2010GL044613.

Cattiaux J, Yiou P, Vautard R. 2012. Dynamics of future seasonal temperature trends and extremes in Europe: A multi-model analysis from CMIP3. Climate Dynamics 38(9–10): 1949–1964. DOI: 10.1007/s00382-011-1211-1.

Connolley WM, Bracegirdle TJ. 2007. An Antarctic assessment of IPCC AR4 coupled models. Geophysical Research Letters 34(22): L22505. DOI: 10.1029/2007GL031648.

De Jongh ILM, Verhoest NEC, De Troch FP. 2006. Analysis Of A 105-year time series of precipitation observed at Uccle, Belgium. International Journal of Climatology 26(14): 2023–2039. DOI: 10.1002/joc.1352.

De Ridder K, Gallée H. 1998. Land Surface–Induced Regional Climate Change in Southern Israel. Journal of applied Meteorology 37: 1470–1485.

Deser C, Knutti R, Solomon S, Phillips AS. 2012a. Communication of the role of natural variability in future North American climate. Nature Climate Change 2(11): 775–779. DOI: 10.1038/nclimate1562.

Deser C, Phillips A, Bourdette V, Teng H. 2012b. Uncertainty in climate change projections: the role of internal variability. *Climate dynamics 38*(3-4): 527-546. DOI:

10.1007/s00382-010-0977-x.

Deser C, Hurrell JW, Phillips AS. 2017. The role of the North Atlantic Oscillation in European climate projections. *Climate dynamics* *49*(9-10): 3141-3157. DOI:10.1007/s00382-016-3502-z.

De Wit MJM, Peeters H a., Gastaud PH, Dewil P, Maeghe K, Baumgart J. 2007. Floods in the Meuse basin: Event descriptions and an international view on ongoing measures. International Journal of River Basin Management 5(4): 279–292. DOI: 10.1080/15715124.2007.9635327.

Doutreloup S, Wyard C, Amory C, Kittel C, Erpicum M, Fettweis X. 2019a. Sensitivity to Convective Schemes on Precipitation Simulated by the Regional Climate Model MAR over Belgium (1987–2017). Atmosphere 10(1): 34. DOI: 10.3390/atmos10010034.

Doutreloup S, Kittel C, Wyard C, Belleflamme A, Amory C., Erpicum M, Fettweis F. 2019b. Precipitation Evolution over Belgium by 2100 and Sensitivity to Convective Schemes Using the Regional Climate Model MAR. Atmosphere 10(321): 15. DOI: 10.3390/atmos10060321.

Driessen TL a., Hurkmans RTWL, Terink W, Hazenberg P, Torfs PJJF, Uijlenhoet R. 2010. The hydrological response of the Ourthe catchment to climate change as modelled

by the HBV model. Hydrology and Earth System Sciences Discussions 14: 651–665. DOI: 10.5194/hessd-6-7143-2009.

Dupriez GL, Sneyers R. 1978. Les normales du réseau pluviométrique belge. Institut royal météorologique de Belgique, Publication Série A 101, 23 p.

Durand Y, Giraud G, Laternser M, Etchevers P, Mérindol L, Lesaffre B. 2009. Reanalysis of 47 Years of Climate in the French Alps (1958–2005): Climatology and Trends for Snow Cover. Journal of Applied Meteorology and Climatology 48(12): 2487–2512. DOI: 10.1175/2009JAMC1810.1.

Dyrrdal AV, Saloranta T, Skaugen T, Stranden HB. 2013. Changes in snow depth in Norway during the period 1961–2010. Hydrology Research 44(1): 169. DOI: 10.2166/nh.2012.064.

Erpicum M, Nouri M, Demoulin A. 2018. The Climate of Belgium and Luxembourg. In: Demoulin A (ed) Landscapes and landforms of Belgium and Luxembourg. Springer Berlin Heidelberg: Cham, 35–41. DOI: 10.1007/978-3-319-58239-9_3.

Falarz MG. 2004. Variability and trends in the duration and depth of snow cover in Poland in the 20th century. International Journal of Climatology 24(13): 1713–1727. DOI: 10.1002/joc.1093.

Fettweis X, Franco B, Tedesco M, van Angelen JH, Lenaerts JTM, van den Broeke MR, Gallée H. 2013. Estimating Greenland ice sheet surface mass balance contribution to future sea level rise using the regional atmospheric climate model MAR. The Cryosphere 7: 469–489. DOI: doi:10.5194/tc-7-469-2013.

Fettweis X, Wyard C, Doutreloup S, Belleflamme A. 2017. Noël 2010 En Belgique : Neige En Flandre Et Pluie En Haute-Ardenne. BSGLg 68(1).

Gallée H. 1995. Simulation of the Mesocyclonic Activity in the Ross Sea, Antarctica. Monthly Weather Review 123: 2051–2069. DOI: https://doi.org/10.1175/1520-0493(1995)123<2051:SOTMAI>2.0.CO;2.

Gallée H, Schayes G. 1994. Development of a Three-Dimensional Meso-Primitive Equation Model: Katabatic Winds Simulation in the Area of Terra Nova Bay, Antarctica. Monthly Weather Review 122(4): 671–685. DOI: 10.1175/1520-0493(1994)122<0671:DOATDM>2.0.CO;2.

Gelaro R, McCarty W, Suárez MJ, Todling R, Molod A, Takacs L, Randles CA, Darmenov A, Bosilovich MG, Reichle R, Wargan K, Coy L, Cullather R, Draper C, Akella S, Buchard V, Conaty A, da Silva AM, Gu W, Kim GK, Koster R, Lucchesi R, Merkova D, Nielsen JE, Partyka G, Pawson S, Putman W, Rienecker M, Schubert SD, Sienkiewicz M, Zhao B. 2017. The modern-era retrospective analysis for research and appli-

cations, version 2 (MERRA-2). Journal of Climate 30(14): 5419–5454. DOI: 10.1175/JCLI-D-16-0758.1.

Gellens D. 2000. Trend and Correlation Analysis of k-Day Extreme Precipitation over Belgium. Theoretical and Applied Climatology 66(1–2): 117–129. DOI: 10.1007/s007040070037.

Hamlet AF, Lettenmaier DP. 2007. Effects of 20th century warming and climate variability on flood risk in the western U.S. Water Resources Research 43(6): 1–17. DOI: 10.1029/2006WR005099.

Hawkins E, Sutton R. 2009. The Potential to Narrow Uncertainty in Regional Climate Predictions. Bulletin of the American Meteorological Society 90(8): 1095-1107. DOI: 10.1175/2009BAMS2607.1.

Hawkins E, Sutton R. 2011. The potential to narrow uncertainty in projections of regional precipitation change. Climate Dynamics 37(1-2): 407-418. DOI: 10.1007/s00382-010-0810-6.

Iversen T, Bentsen M, Bethke I, Debernard JB, Kirkevåg A, Seland Ø, Drange H, Kristjánsson JE, Medhaug I, Sand M, Seierstad IA. 2012. The Norwegian Earth System Model, NorESM1-M – Part 2: Climate response and scenario projections. Geoscientific Model Development Discussions 5(3): 2933–2998. DOI: 10.5194/gmdd-5-2933-2012.

Journée M, Delvaux C, Bertrand C. 2015. Precipitation climate maps of Belgium. Advances in Science and Research 12: 73–78. DOI: 10.5194/asr-12-73-2015.

Kay AL. 2016. A review of snow in Britain: The historical picture and future projections. Progress in Physical Geography. DOI: 10.1177/0309133316650617.

Kittel C, Amory C, Agosta C, Delhasse,A, Doutreloup S, Huot, PV, Wyard C, Fichefet T, Fettweis X. 2018. Sensitivity of the current Antarctic surface mass balance to sea surface conditions using MAR. Cryosphere 12: 3827–3839.

Kjellström E, Thejll P, Rummukainen M, Christensen JH, Boberg F, Christensen OB, Maule CF. 2013. Emerging regional climate change signals for Europe under varying large-scale circulation conditions. Climate Research 56(2): 103-119. DOI: 10.3354/cr01146.

Lang C, Fettweis X, Erpicum M. 2015. Future climate and surface mass balance of Svalbard glaciers in an RCP8.5 climate scenario: a study with the regional climate model MAR forced by MIROC5. The Cryosphere 9(3): 945–956. DOI: 10.5194/tc-9-945-2015.

Legras B, Ghil M. 1985. Persistent Anomalies, Blocking and Variations in Atmospheric Predictability. Journal of the Atmospheric Sciences 42(5): 433–471. DOI: 10.1175/1520-0469(1985)042<0433:PABAVI>2.0.CO;2.

Madsen H, Lawrence D, Lang M, Martinkova M, Kjeldsen TR. 2014. Review of trend analysis and climate change projections of extreme precipitation and floods in Europe. Journal of Hydrology. Elsevier B.V. 519(PD): 3634–3650. DOI: 10.1016/j.jhydrol.2014.11.003.

McSweeney CF, Jones RG, Lee RW, Rowell DP. 2015. Selecting CMIP5 GCMs for downscaling over multiple regions. Climate Dynamics 44(11-12): 3237-3260. DOI: 10.1007/s00382-014-2418-8.

Murphy JM, Sexton DMH, Barnett DN, Jones GS, Webb MJ, Collins M, Stainforth DA. 2004. Quantification of modelling uncertainties in a large ensemble of climate change simulations. Nature 430(7001): 768–772. DOI: 10.1038/nature02771.

Ntegeka V, Willems P. 2008. Trends and multidecadal oscillations in rainfall extremes, based on a more than 100-year time series of 10 min rainfall intensities at Uccle, Belgium. Water Resources Research 44(7): 1–15. DOI: 10.1029/2007WR006471.

Petit F, Pauquet A. 1997. Bankfull discharge recurrence interval in gravel-bed rivers. Earth Surface Processes 22: 685–693. DOI: 10.1002/(SICI)1096-9837(199707)22:7<685::AID-ESP744>3.0.CO;2-J.

Perez J, Menendez M, Mendez FJ, Losada IJ. 2014. Evaluating the performance of CMIP3 and CMIP5 global climate models over the north-east Atlantic region. Climate

Dynamics 43(9-10): 2663-2680. DOI:10.1007/s00382-014-2078-8.

Prein AF, Pendergrass AG. 2019. Can We Constrain Uncertainty in Hydrologic Cycle Projections? Geophysical Research Letters 46(7): 3911-3916. DOI: 10.1029/2018GL081529.

Reinhold BB, Pierrehumbert RT. 1982. Dynamics of Weather Regimes: Quasi-Stationary Waves and Blocking. Monthly Weather Review 110(9): 1105–1145. DOI: 10.1175/1520-0493(1982)110<1105:DOWRQS>2.0.CO;2.

RMIB. 2015. Vigilance Climatique. Royal Meteorological Institute of Belgium: Brussels.

Saeed S, Brisson E, Demuzere M, Tabari H, Willems P, van Lipzig NPM. 2017. Multidecadal convection permitting climate simulations over Belgium: sensitivity of future precipitation extremes. Atmospheric Science Letters 18(1): 29–36. DOI: 10.1002/asl.720.

Skaugen T, Stranden HB, Saloranta T. 2012. Trends in snow water equivalent in Norway (1931–2009). Hydrology Research 43(4): 489. DOI: 10.2166/nh.2012.109.

Sneyers R, Vandiepenbeeck M, Vanlierde R. 1989. Principal component analysis of belgian rainfall. Theor. Appl. Climatol. 39(4): 199–204.

Stewart IT. 2009. Changes in snowpack and snowmelt runoff for key mountain regions. Hydrological Processes 23(1): 78–94. DOI: 10.1002/hyp.7128.

Tabari H, Taye MT, Willems P. 2015. Water availability change in central Belgium for the late 21st century. Global and Planetary Change. Elsevier B.V. 131: 115–123. DOI: 10.1016/j.gloplacha.2015.05.012.

Taylor KE, Stouffer RJ, Meehl GA. 2012. An Overview of CMIP5 and the Experiment Design An Overview of CMIP5 and the Experiment Design. Bulletin of the American Meteorological Society 93(4): 485–498.

Vaes G, Willems P BJ. 2002. 100 years of Belgian rainfall: are there trends? Water Sci. Technol. 45(2): 55–61.

Valt M, Cianfarra P. 2010. Recent snow cover variability in the Italian Alps. Cold Regions Science and Technology. Elsevier B.V. 64(2): 146–157. DOI: 10.1016/j.coldregions.2010.08.008.

Van de Vyver H. 2012. Evolution of extreme temperatures in Belgium since the 1950s. Theoretical and Applied Climatology 107(1–2): 113–129. DOI: 10.1007/s00704-011-0456-2.

Van Meijgaard E. 1995. Excessive rainfall over the belgian ardennes in december 1993:

evaluation of model predictions. Meteorol. App. 2(1): 39–52.

Van Uytven E, Willems P. 2018. Greenhouse gas scenario sensitivity and uncertainties in precipitation projections for central Belgium. Journal of Hydrology. Elsevier B.V. 558: 9–19. DOI: 10.1016/j.jhydrol.2018.01.018.

Vanden Broucke S, Wouters H, Demuzere M, van Lipzig NPM. 2018. The influence of convection-permitting regional climate modeling on future projections of extreme precipitation: dependency on topography and timescale. Climate Dynamics. Springer Berlin Heidelberg 0(0): 0. DOI: 10.1007/s00382-018-4454-2.

Vaughan DG, Comiso JC, Allison I, Carrasco J, Kaser G, Kwok R, Mote P, Murray T, Paul F, Ren J, Rignot E, Solomina O, Steffen K, Zhang T. 2013. Observations: Cryosphere. Climate Change 2013: The Physical Science Basis. Contribution of Working Group I to the Fifth Assessment Report of the Intergovernmental Panel on Climate Change.

Vautard R. 1990. Multiple Weather Regimes over the North Atlantic: Analysis of Precursors and Successors. Monthly Weather Review 118(10): 2056–2081. DOI: 10.1175/1520-0493(1990)118<2056:MWROTN>2.0.CO;2.

von Trentini F, Leduc M, Ludwig R. 2019. Assessing natural variability in RCM signals: comparison of a multi model EURO-CORDEX ensemble with a 50-member single

model large ensemble. Climate Dynamics 53(3-4): 1963-1979. DOI:10.1007/s00382-019-04755-8.

Vormoor K, Lawrence D, Schlichting L, Wilson D, Wong WK. 2016. Evidence for changes in the magnitude and frequency of observed rainfall vs. snowmelt driven floods in Norway. JOURNAL OF HYDROLOGY. Elsevier B.V. 538: 33–48. DOI: 10.1016/j.jhydrol.2016.03.066.

Watanabe M, Suzuki T, O'ishi R, Komuro Y, Watanabe S, Emori S, Takemura T, Chikira M, Ogura T, Sekiguchi M, Takata K, Yamazaki D, Yokohata T, Nozawa T, Hasumi H, Tatebe H, Kimoto M. 2010. Improved Climate Simulation by MIROC5: Mean States, Variability, and Climate Sensitivity. Journal of Climate 23(23): 6312–6335. DOI: 10.1175/2010JCLI3679.1.

Willems P. 2013a. Revision of urban drainage design rules after assessment of climate change impacts on precipitation extremes at Uccle, Belgium. Journal of Hydrology. Elsevier B.V. 496: 166–177. DOI: 10.1016/j.jhydrol.2013.05.037.

Willems P. 2013b. Multidecadal oscillatory behaviour of rainfall extremes in Europe. Climate Change 120: 931–944. DOI: 10.1007/s10584-013-0837-x.

Wyard C, Doutreloup S, Belleflamme A, Wild M, Fettweis X. 2018. Global Radiative Flux and Cloudiness Variability for the Period 1959–2010 in Belgium: A Comparison

between Reanalyses and the Regional Climate Model MAR. Atmosphere 9(7): 262. DOI: 10.3390/atmos9070262.

Wyard C, Scholzen C, Fettweis X, Van Campenhout J, François L. 2017. Decrease in climatic conditions favouring floods in the south-east of Belgium over 1959-2010 using the regional climate model MAR. International Journal of Climatology 37(5): 2782–2796. DOI: 10.1002/joc.4879.

Zamani S, Gobin A, Van de Vyver H, Gerlo J. 2016. Atmospheric drought in Belgium - statistical analysis of precipitation deficit. International Journal of Climatology 36(8): 3056–3071. DOI: 10.1002/joc.4536.

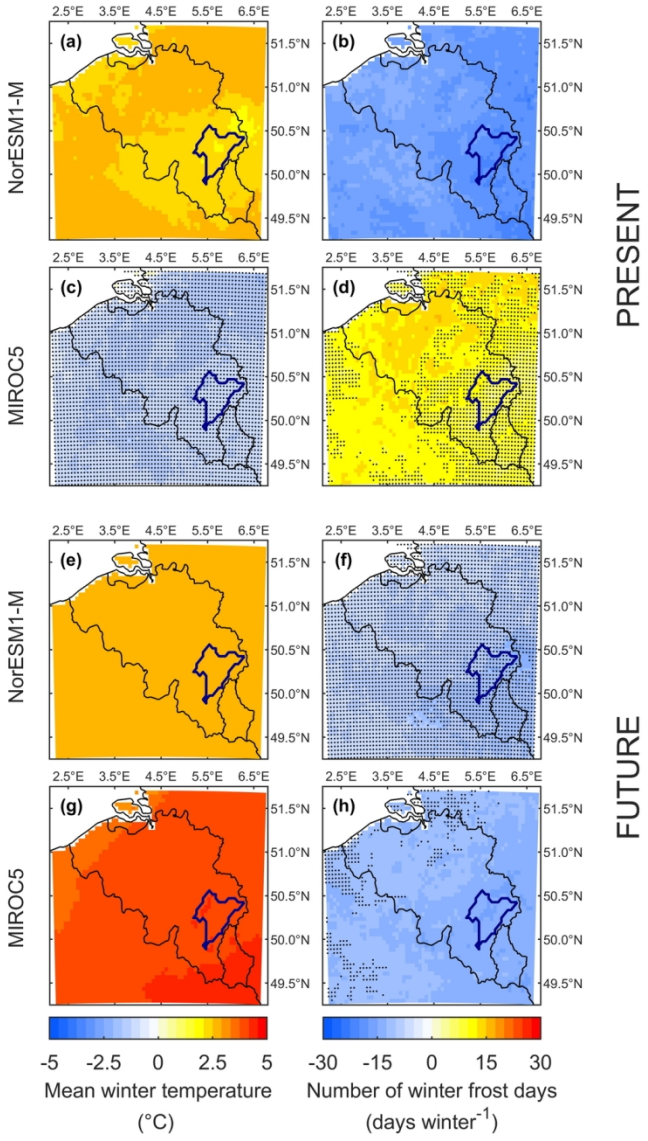

Figure 1. (Top) Present-day anomalies of MAR forced by NorESM1-M and MIROC5 with respect to MAR forced by ERA40/ERA-interim during the winter months (December-January-February) over 1976-2005 regarding (a, c) the mean winter temperature, (b, d) the number of winter frost days. (Bottom) Future changes simulated by MAR forced by NorESM1-M and MIROC5 over 2071-2100 during the winter months (December-January-February) with respect to 1976-2005 regarding (e, g) the mean winter temperature, (f, h) the number of winter frost days. Stippling pixels indicate anomalies/changes that are statistically non-significant with respect to the interannual variability of the reference field.

120x165mm (300 x 300 DPI)

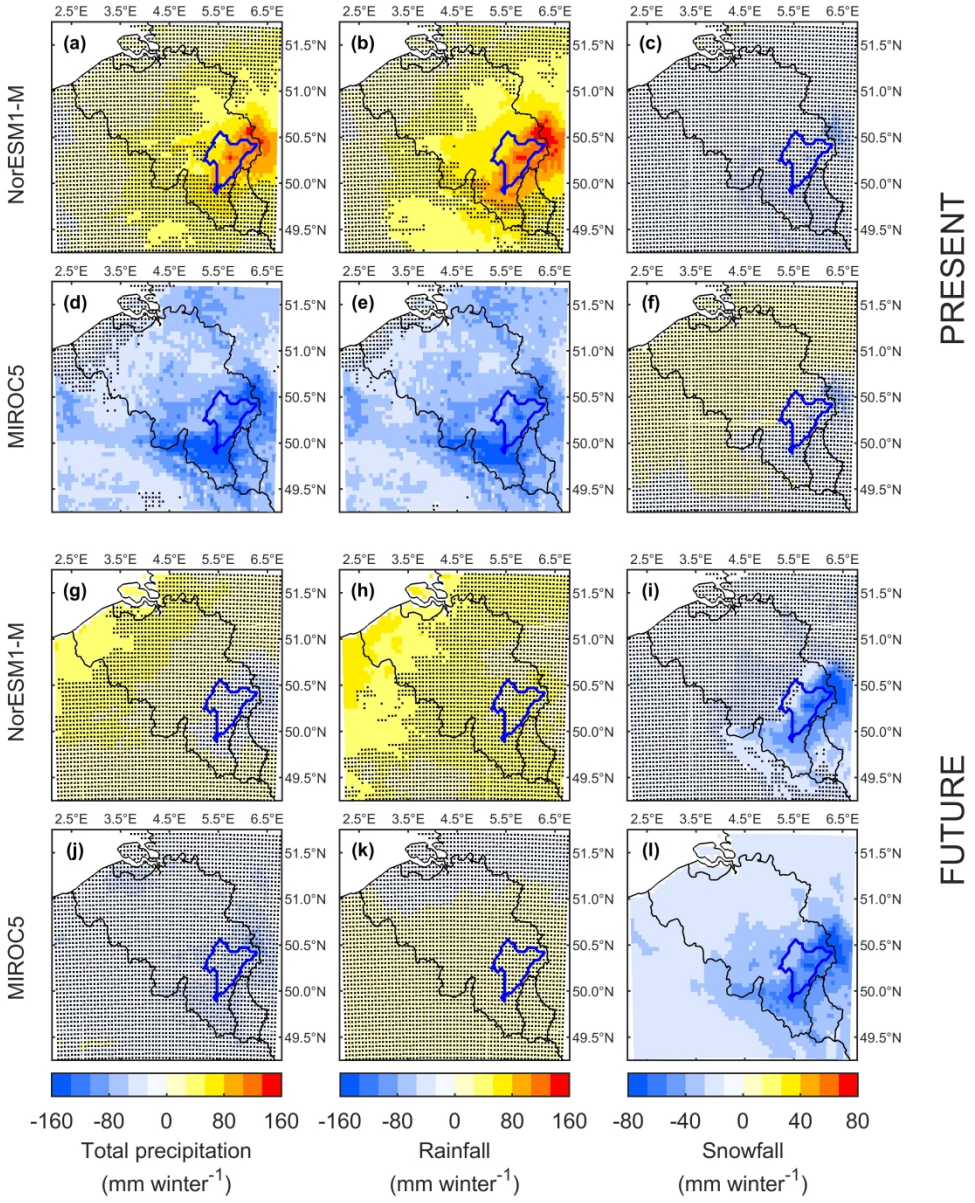

Figure 2. (Top) Present-day anomalies of MAR forced by NorESM1-M and MIROC5 with respect to MAR forced by ERA40/ERA-interim during the winter months (December-January-February) over 1976-2005 regarding (a, d) total precipitation, (b, e) rainfall amount, and (c, f) snowfall amount. (Bottom) Future changes simulated by MAR forced by NorESM1-M and MIROC5 over 2071-2100 during the winter months (December-January-February) with respect to 1976-2005 regarding (g, j) total precipitation, (h, k) rainfall amount, and (i, l) snowfall amount. Stippling pixels indicate anomalies/changes that are statistically non-significant with respect to the interannual variability of the reference field.

127x156mm (599 x 599 DPI)

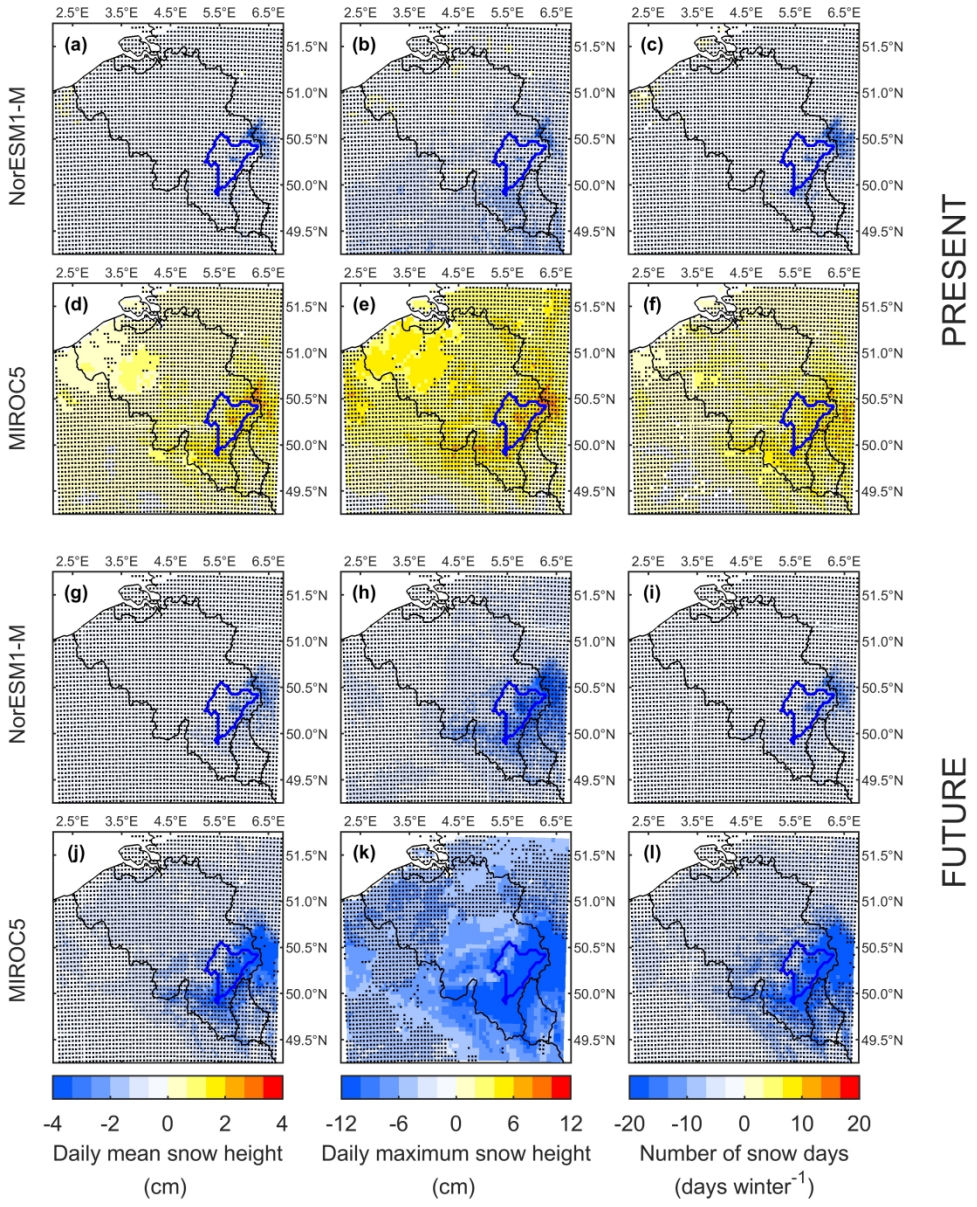

Figure 3. (Top) Present-day anomalies of MAR forced by NorESM1-M and MIROC5 with respect to MAR forced by ERA40/ERA-interim during the winter months (December-January-February) over 1976-2005 regarding (a, d) the daily mean snow height, (b, e) the daily maximum snow height, and (c, f) the number of snow days. (Bottom) Future changes simulated by MAR forced by NorESM1-M and MIROC5 over 2071-2100 during the winter months (December-January-February) with respect to 1976-2005 regarding (g, j) the daily mean snow height, (h, k) the daily maximum snow height, and (i, l) the number of snow days. Stippling pixels indicate anomalies/changes that are statistically non-significant with respect to the interannual variability of the reference field.

127x156mm (599 x 599 DPI)

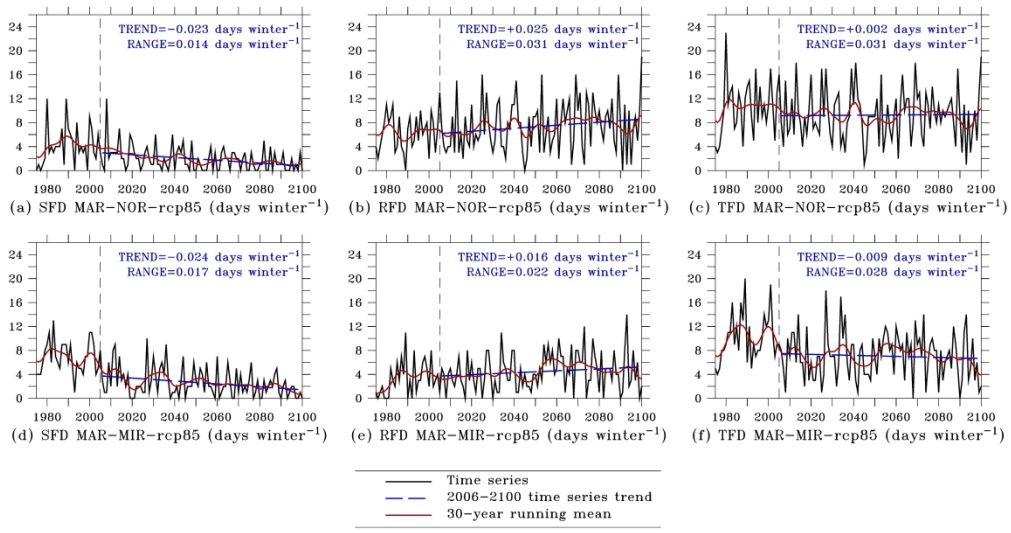

Figure 4. Time series (black lines), 30-year running mean (red lines), and trends (blue lines) computed from MAR-NOR-rcp85 and MAR-MIR-rcp85 of (a, d) the number of days favourable to floods dominated by to snowpack melting (SFD), (b, e) the number of days favourable to floods dominated by rainfall (RFD), and (c, f) the total number of days favourable to floods (TFD), during the winter months (December-January-February).

185x97mm (500 x 500 DPI)

Table 1. Simulations performed with MAR for the use of this study.

Short name	Run type	Forcing	Run Period
MAR-ERA	Historical	ERA40/ERA-interim	1976-2005
MAR-MIR-histo	Historical	MIROC5-histo	1976-2005
MAR-MIR-rcp85	Projection	MIROC5-rcp85	2006-2100
MAR-NOR-histo	Historical	NorESM1-M-histo	1976-2005
MAR-NOR-rcp85	Projection	NorESM1-M-rcp85	2006-2100

Table 2. Average number of days favourable to floods per winter due to snowpack melting (SFD) and due to rainfall (RFD) as well as the total average number of days favourable to floods (TFD=SFD+RFD) modelled by MAR-ERA, MAR-NOR-histo and MAR-MIR-histo over 1976-2005.

Simulation	SFD [days winter^{-1}]	RFD [days winter^{-1}]	TFD [days winter^{-1}]
MAR-ERA (MARv3.6)	5.0 ± 4.8	5.6 ± 4.9	10.6 ± 7.4
MAR-ERA	4.2 ± 3.5	5.5 ± 3.0	9.7 ± 3.9
MAR-NOR-histo	4.3 ± 3.1	6.6 ± 3.2	10.9 ± 4.5
MAR-MIR-histo	7.0 ± 2.7	3.5 ± 2.9	10.5 ± 3.9

Table 3. Average number of days favourable to floods per winter due to snowpack melting (SFD) and due to rainfall (RFD) as well as the total average number of days favourable to floods (TFD=SFD+RFD) modelled by MAR-ERA, MAR-NOR-histo and MAR-MIR-histo for the period 2071-2100.

Simulation	SFD [days winter^{-1}]	RFD [days winter^{-1}]	TFD [days winter^{-1}]
MAR-NOR-rcp85	**1.2[1] (-73%)[2]**	8.3 (+26%)	9.5 (-13%)
MAR-MIR-rcp85	**1.8 (-74%)**	4.8 (+39%)	**6.6 (-37%)**

[1] The values in bold are statistically significant
[2] The values under brackets refer to relative changes with respect to 1976-2005